Electronic Supplementary Material (ESI) for ChemComm.

Electronic Supplementary Information

Bubble-Induced Transport of Oil Droplets in Water

Ying Chu and Qinmin Pan*

(*State Key Laboratory of Robotics and Systems, School of Chemical Engineering and Technology, Harbin Institute of Technology, Harbin 150001, P. R. China*)

E–mail: panqm@hit.edu.cn

EXPERIMENTAL SECTION

Instrumental Techniques

X–ray photoelectron spectroscopy (XPS) was measured by using a PHI–5700 ESCA. Transmission electron microscopy (TEM) images were recorded on an H–7650 (Hitachi). Scanning electron microscopy (SEM) observations were conducted on a FEI Sirion 200. A digital microscope (VHX–500, Keyence) was used to *in situ* record the two-dimensional (2D) and three-dimensional (3D) images of the encapsulated $CHCl_3$ droplets in water. The formation and growth of "airbags" was also observed by the CCD camera of an OCA–20 (DataPhysics Instruments).

Materials

Ethanol (99.7%), tetraethoxysilane ($C_8H_{20}O_4Si$, TEOS), ammonia solution ($NH_3 \cdot H_2O$, 25 wt%), styrene, potassium peroxydisulfate ($K_2S_2O_8$), ferric trichloride hexahydrate ($FeCl_3 \cdot 6H_2O$), ethylene glycol, sodium acetate trihydrate ($NaAc \cdot 3H_2O$), nitric acid (HNO_3), cerium (IV) ammonium nitrate ($Ce(NH_4)_2(NO_3)_6$, CAN), *N*-isopropylacrylamide (NIPAm), *N, N'*-methylenebisacrylamide (MBA), tetramethyl ethylenediamine (TMEDA) and ammonium persulfate (APS) were provided by Tianjin Kermel Chemical Reagent Co., Ltd. (China).

Synthesis of SiO_2-PNIPAm Nanoparticles

At first, SiO_2 nanoparticles (~500 nm in diameter) were synthesized according to the procedure described in reference.[1] Typically, 16 mL of ethanol, 25 mL of deionized water and 9 mL of $NH_3 \cdot H_2O$ (25 wt%) were mixed to form a colorless solution. Then tetraethoxysilane (TEOS, 4.5 mL) and ethanol (45.5 mL) were added to the above solution quickly. After stirring for 5 h, the resulting mixture was separated by centrifugation and the solid residue was dried at 120 ^oC to obtain SiO_2 nanoparticles.

The resulting SiO_2 nanoparticles (50 mg) were dispersed in 25 mL of deionized water by sonication. Then 0.5 mL of HNO_3, 500 mg of *N*-isopropylacrylamide (NIPAm), and 15 mg of *N*, *N'*-methylenebisacrylamide (MBA)

were added to the above dispersion in argon atmosphere. Later, 1 g of cerium (IV) ammonium nitrate[2] and 4 μL of tetramethyl ethylenediamine (TMEDA) were added to the dispersion. The resultant mixture was kept stirring for 12 h in argon atmosphere. After reaction, white powder (SiO_2-PNIPAm nanoparticles) was collected by centrifugation and then washed with deionized water five times. The resulting SiO_2-PNIPAm nanoparticles were dipped in deionized water overnight to leach out unreacted reagents.

Synthesis of polystyrene (PS) nanoparticles

PS nanoparticles were synthesized according the procedure described in reference.[3] Briefly, styrene monomer (30 mL, distilled before use) was added to deionized water (250 mL) by vigorously stirring at 70 ^oC for 30 min in argon atmosphere. Then 0.52 g of potassium peroxydisulfate ($K_2S_2O_8$) was added to the above dispersion. After polymerization for 20 h, the resultant white emulsion was separated by centrifugation and the solid residue was washed with deionized water five times. PS nanoparticles with ~500 nm in diameter were obtained after drying at 100 ^oC.

Synthesis of Fe_3O_4 nanoparticles

$FeCl_3 \cdot 6H_2O$ (1.35 g) and $NaAc \cdot 3H_2O$ (3.6 g) were added to 40 mL of ethylene glycol by stirring. The resulting mixture was sealed in a teflon-lined stainless steel autoclave and heated at 200 ^oC for 18 h. After cooling to room temperature, the black powder was collected by a magnetic bar and subsequently washed with ethanol and water five times. Fe_3O_4 nanoparticles (~300 nm in diameter) were obtained after drying at 60 ^oC.[4]

Synthesis of PS-PNIPAm and Fe_3O_4-PNIPAm nanoparticles

At first, 50 mg of PS nanoparticles were treated with ultraviolet/ozone (UV/O_3) for 2 h. The resulting PS nanoparticles or Fe_3O_4 nanoparticles (50 mg) were added to deionized water (25 mL) by sonication. Then *N*-isopropylacrylamide (NIPAm, 500 mg), HNO_3 (0.5 mL), and *N*, *N'*-methylenebisacrylamide (MBA, 15 mg) were added to the above mixtures under stirring in argon atmosphere. Later, cerium (IV) ammonium nitrate[2] (CAN, 1 g)

and tetramethyl ethylenediamine (TMEDA, 4 μL) were added to the resulting dispersion. After stirring in argon atmosphere for 12 h, the resultant dispersion was separated by centrifugation. The solid residue was then washed with deionized water five times to obtain PS-PNIPAm or Fe_3O_4-PNIPAm nanoparticles.

Synthesis of pure PNIPAm hydrogel

4 mL of deionized water, 200 mg of NIPAm and 6 mg of MBA were added to a three-necked flask in argon. After stirring for 30 min, 20 mg of ammonium persulfate (APS) and 4 μL of TMEDA were added to the above mixture quickly. The mixture was kept stirring in argon for 1 h.[5] The resulting PNIPAm hydrogel was dialyzed in deionized water for one day to leach out unreacted reagents.

Transportation of $CHCl_3$ Droplets in Water

In a typical experiment, SiO_2-PNIPAm nanoparticles were dispersed in 10 mL of water. After sedimentation for 5 h, a film of SiO_2-PNIPAm nanoparticles was formed on the water bottom. A droplet of $CHCl_3$ (6 μL) containing Sudan red (~6 μg) was placed on the film. By gently shaking, the surface of the droplet was encapsulated with a layer of SiO_2-PNIPAm nanoparticles.[6,7] The size of $CHCl_3$ droplets was controlled by a pipettor. After water temperature was increased to 33.0 ^oC, a tiny "airbag" was formed on the top of the encapsulated droplet. As the "airbag" grew, the droplet vertically transported to the water surface. After stayed at the water surface for ~15 s, the "airbag" broken and the droplet fell to the water bottom. Then the temperature was decreased to 25.0 ^oC, which allowed self-healing of the broken encapsulating layer. When the temperature was increased to 33.0 ^oC, an "airbag" was formed again and the droplet was able to transport in water once more. The droplet could repeat the ascent and descent process three times in this case.

Intelligent Delivery of a Small Amount of Lipophilic Moiety in Water

At first, a $CHCl_3$ (6 μL) droplet containing ~6 μg of Sudan red was encapsulated with a layer of SiO_2-PNIPAm nanoparticles in water, according to the procedure described above. Then the surface of water was covered with a

layer of blue-dyed *n*-dodecane. As the temperature rose to 33.0 ^{o}C, the droplet transported to the water surface. Then Sudan red was released from the droplet as its "airbag" broken at the water surface. The released dye was absorbed by the *n*-dodecane layer, which dyed the layer purple.

In another experiment, no loss transportation of Sudan red was conducted as follows. At first, a $CHCl_3$ (6 μL) droplet containing ~6 μg of Sudan red was encapsulated with a layer of SiO_2-PNIPAm nanoparticles in water. Then a piece of superhydrophobic sponge was placed on the water surface. As the temperature rose to 33.0 ^{o}C, the droplet ascended to the water surface where it was completed absorbed by the sponge. The superhydrophobic sponge was fabricated according to the procedure described in reference.[8,9]

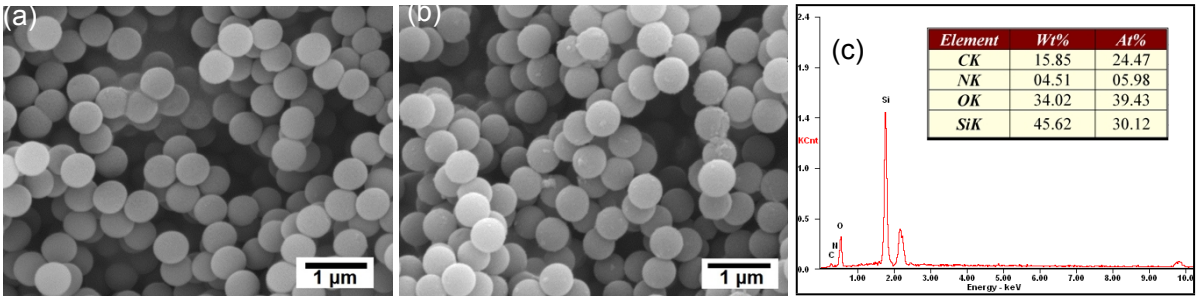

Fig. S1. SEM images for the pristine SiO_2 (a) and SiO_2-PNIPAm (b) nanoparticles. (c) EDX plot of SiO_2-PNIPAm nanoparticles.

Fig. S1 is the SEM image and EDX plot for SiO_2-PNIPAm nanoparticles. Compared with the pristine SiO_2 nanoparticles (Fig. S1a), SiO_2-PNIPAm nanoparticles exhibit a rough appearance (Fig. S1b). Moreover, EDX plot also shows the presence of N element for SiO_2-PNIPAm (Fig. S1c).

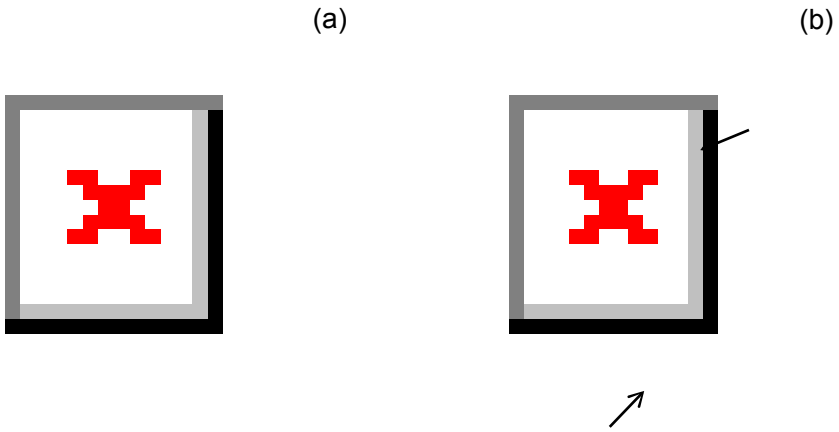

Fig. S2. TEM images of the pristine SiO_2 (a) and SiO_2-PNIPAm (b) nanoparticles.

Fig. S2 shows the TEM images of the pristine SiO_2 and SiO_2-PNIPAm nanoparticles. Unlike smooth surface of the pristine SiO_2 nanoparticles, SiO_2-PNIPAm nanoparticles exhibit a rough mophology. These results are consistent with those of SEM observation, indicting the grafting of poly(*N*-isopropylacrylamide) to the surface of SiO_2 nanoparticles.

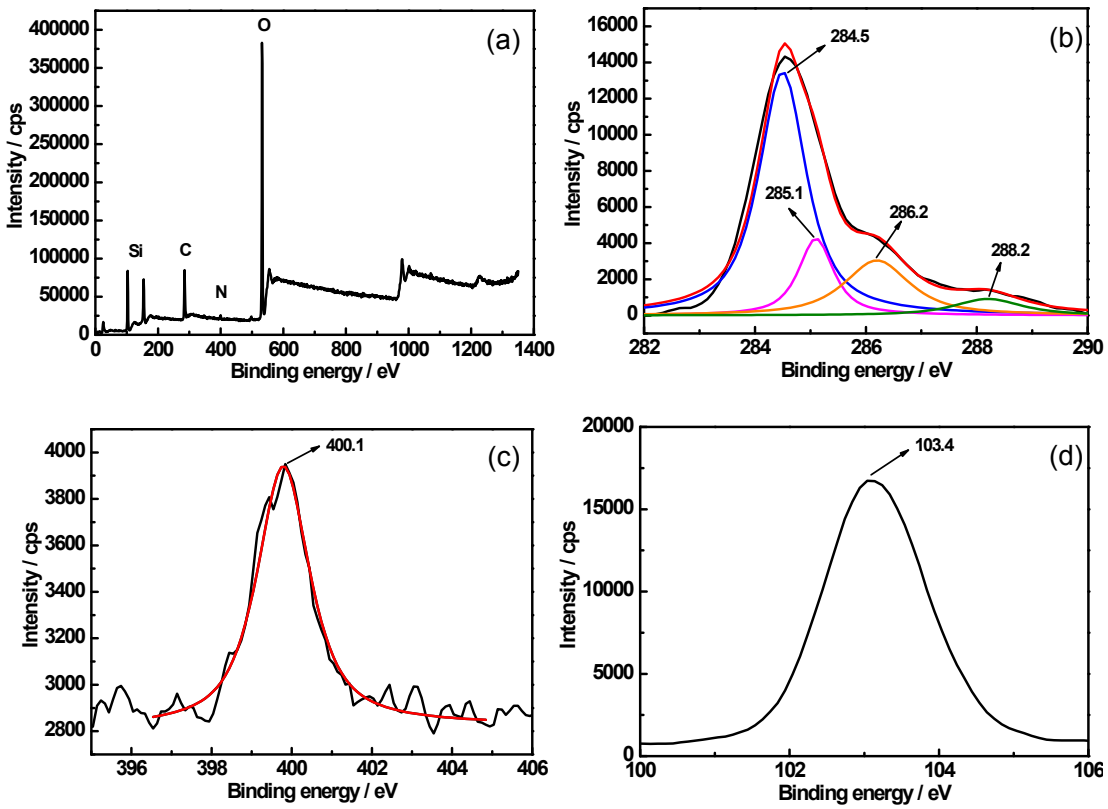

Fig. S3. XPS results of SiO_2-PNIPAm nanoparticles. (a) Survey scan, (b) C 1s, (c) N 1s and (d) Si 2p.

The chemical structure of SiO_2-PNIPAm nanoparticles was identified by XPS (Fig. S3). The survey scan shows the elements of Si, C, O, and N (Fig. S3a). In C 1s spectrum, there are four peaks located at 284.5, 285.1, 286.2 and 288.2 eV (Fig. S3b), which can be attributed to the C atoms of $–CH_3$, –C–C=O, C–N, and HN–C=O, respectively.[10,11] The presence of amide component was also confirmed by the N 1s spectrum (Fig. S3c) because a peak ascribed to HN–C=O is observed at 400.1 eV. For Si 2p spectrum, only a strong peak assigned to SiO_2 is located at 103.4 eV (Fig. S3d). Since the nanoparticles were thoroughly washed with deionized water, XPS results suggest the grafting of poly(*N*-isopropylacrylamide) to SiO_2 nanoparticles.

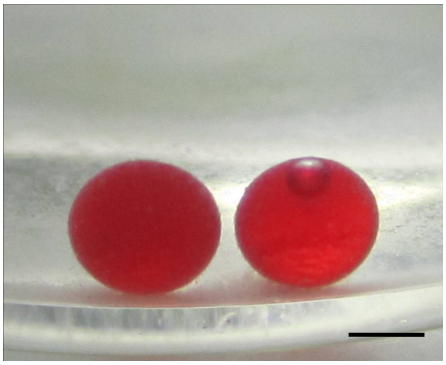

Fig. S4. Optical image of the $CHCl_3$ droplets encapsulated with the pristine SiO_2 (left) and SiO_2-PNIPAm (right) nanoparticles in water at 33.0 °C. The image was recorded after the droplets were placed in water for 6 min. Scale bar: 1 mm.

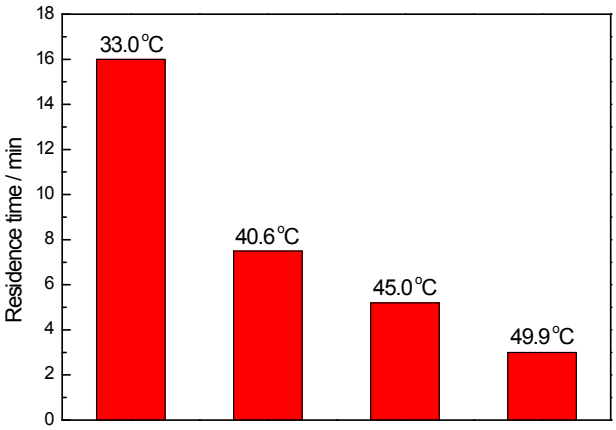

Fig. S5. Effect of temperature on the residence time of encapsulated $CHCl_3$ droplets at the water bottom.

The transportation process could be accelerated by increasing water temperature. To investigate this accelerating effect, we measured the residence time of encapsulated droplets (6 μL) at the water bottom at 33, 40.6, 45.0 and 49.9 °C, respectively. At 33 °C, an encapsulated $CHCl_3$ droplet stayed at the bottom for ~16 min before transportation. In comparison, the time was shortened to ~7.5 and ~3 min when the temperature was 40.6 and 49.9 °C, respectively (Fig. S5).

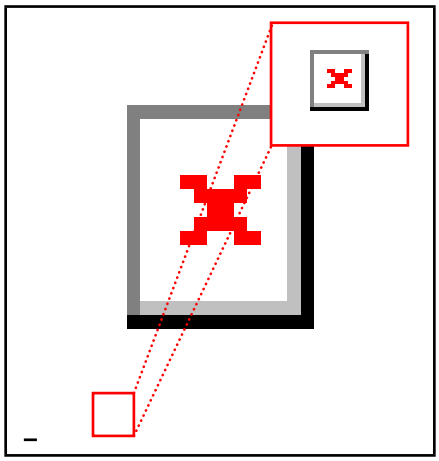

Fig. S6. Control experiment conducted on an encapsulated $CHCl_3$ droplet under degassed conditions. The optical image was taken after the encapsulated droplet stayed in water at 33.8 °C for 20 min. Scale bar: 2 mm.

In order to verify the gas source for "airbags", a control experiment was carried out on a $CHCl_3$ droplet under degassed conditions. Typically, 50 mg of SiO_2-PNIPAm nanoparticles and 10 mL of water were sealed in a glass bottle and then degassed by a vacuum pump for 4 h. Then a droplet of $CHCl_3$ (6 μL) was quickly added to the degassed mixture. After complete encapsulation with SiO_2-PNIPAm nanoparticles, the water temperature was increased to 33.8 °C. It was found that the encapsulated $CHCl_3$ droplet still stayed at the bottom of water, while no "airbag" was observed on its top within 20 min (Fig. S6).

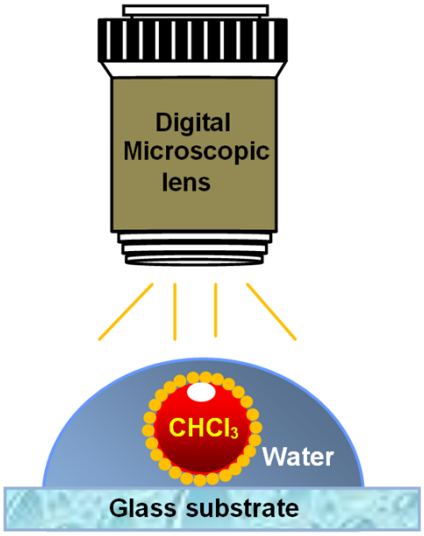

Fig. S7. Illustration for the *in-situ* observation of morphology evolution of an encapsulated droplet in water at 33.0 °C.

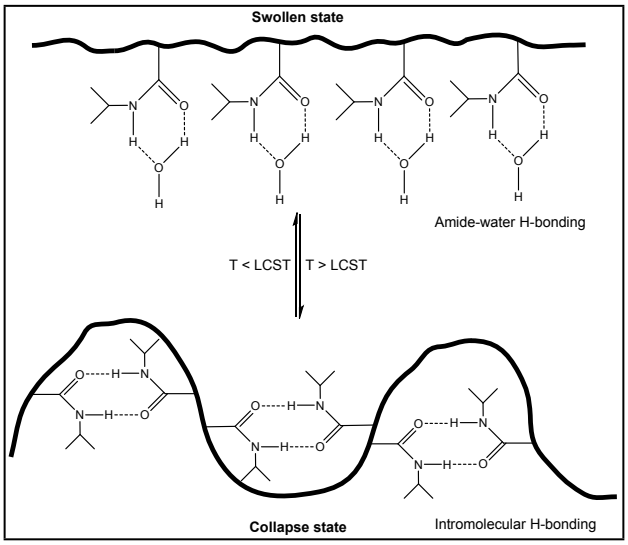

Scheme S1. Illustration for conformation change of poly(*N*-isopropylacrylamide) chains from the swollen state and the collapse state.

Scheme S1 illustrates the conformation change of poly(*N*-isopropylacrylamide) (PNIPAm) chains at different temperature. The conformation change of PNIPAm chains is caused by different types of H-bonding below and above the lower critical solution temperature (LCST).[12-16] Below the LCST, intermolecular H-bonding is formed between C=O and N–H groups of PNIPAm chains and H_2O molecules, allowing the chains to be expanded in water (*i.e.*, swollen conformation). Above the LCST, however, intramolecular H-bonding is formed between the C=O and N–H groups of PNIPAm chains. The intramolecular H-bonding makes hydrophilic C=O and N–H groups far from water, while hydrophobic alkyl segments face water, resulting in the shrinkage of the polymer chains (*i.e.*, collapse conformation).

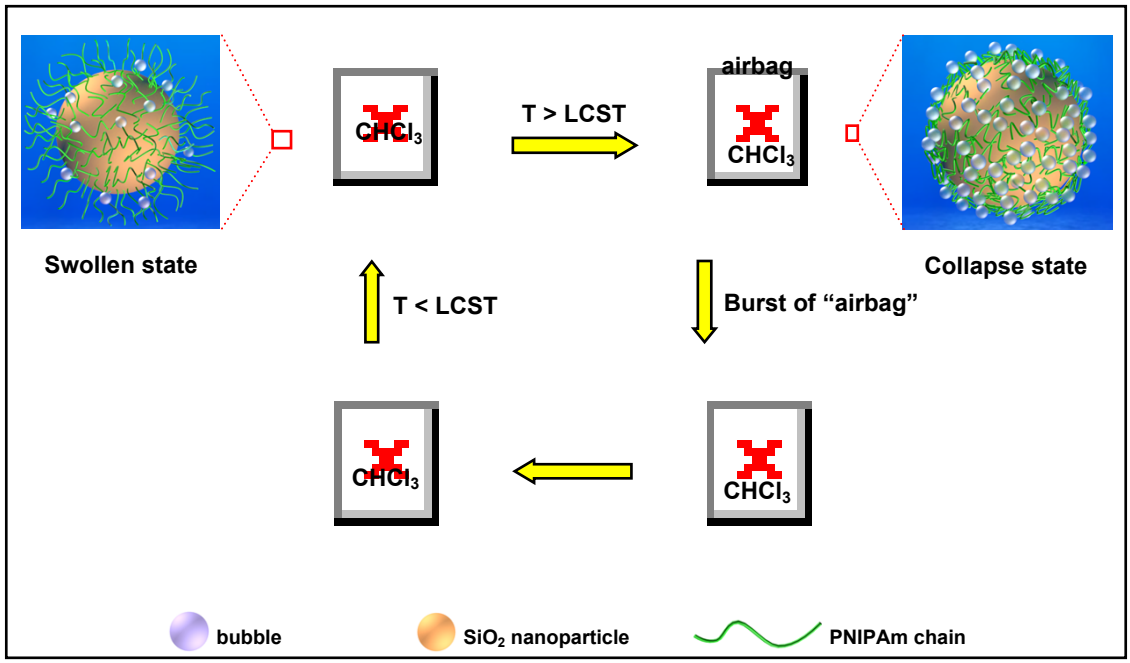

Fig. S8. Illustration for the formation and regeneration of an "airbag" on the encapsulated $CHCl_3$ droplet.

Herein, we propose a mechanism for the formation of an "airbag". On one hand, the surface of SiO_2 nanoparticles is grafted with thermal-responsive PNIPAm whose chains will undergo conformation change below or above the LCST (Scheme S1).[12-16] Below the LCST, PNIPAm chains are at the swollen state and trap a large amount of water. Above the LCST, PNIPAm chains shrink to the collapse state. The shrinkage induces not only the loss of water and any co-solutes but also the assembly (or organization) of SiO_2-PNIPAm nanoparticles on $CHCl_3$.[17,18] The later process results in a compact encapsulating layer on the droplet, as shown in Fig. 2f and Fig. S8. On the other hand, with the shrinkage of PNIPAm chain above LCST, a lot of small bubbles are formed on the surface of PNIPAm hydrogel.[19-25] Owing to the existence of the compact encapsulating layer, these bubbles cannot permeate through the layer. As a result, the bubbles preferentially accumulate on the inner surface of the layer. After continuous accumulation of small bubbles, a larger bubble is formed between $CHCl_3$ and the layer (Fig. S8), resulting in an "airbag" that lifts the droplet to the water surface. Indeed, the formation of bubbles was also observed on the surface of a pure PNIPAm hydrogel at 33.0 ^{o}C, as shown by the optical images in Fig. S9.

The regeneration of the "airbag" is associated with self-healing of the broken SiO_2-PNIPAm encapsulating

layer. Below the LCST, the grafted PNIPAm chains change their conformation into the swollen state and re-trap a large amount of water[12-16] (Scheme S1). The conformation change induces the re-organization of SiO_2-PNIPAm nanoparticles at the $CHCl_3$/water interface. This re-organization process also gives rise to the entanglement of PNIPAm chains between adjacent nanoparticles. All these allow the broken encapsulating layer to repair itself in water at 25 °C. Consequently, an "airbag" regenerates on the droplet once the temperature is above the LCST again (Fig. S8). Although detail mechanism for the growth of an "airbag" deserves further investigations, we believe it is related to the formation of a compact encapsulating layer and the accumulation of bubbles at the interface of $CHCl_3$ and the layer.

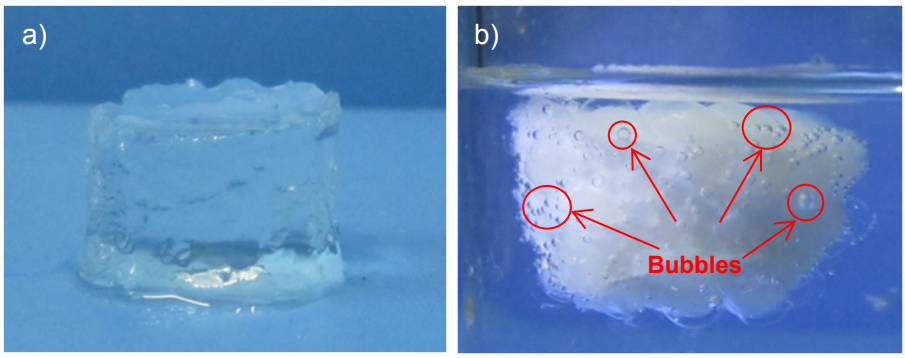

Fig. S9. Optical images of a pure PNIPAm hydrogel placed in (a) air at 25 °C and (b) water at 33 °C.

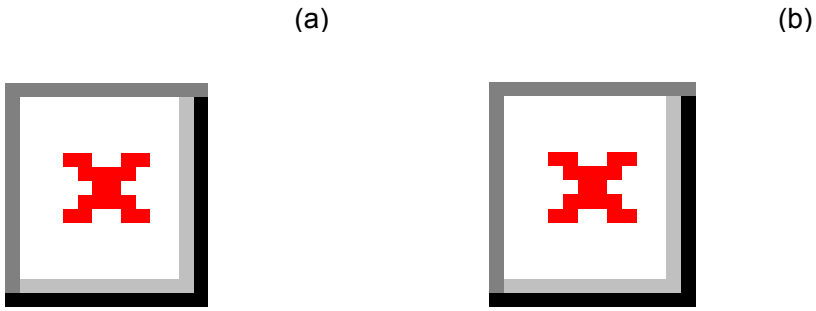

Fig. S10. TEM images of (a) Fe_3O_4-PNIPAm and (b) PS-PNIPAm nanoparticles.

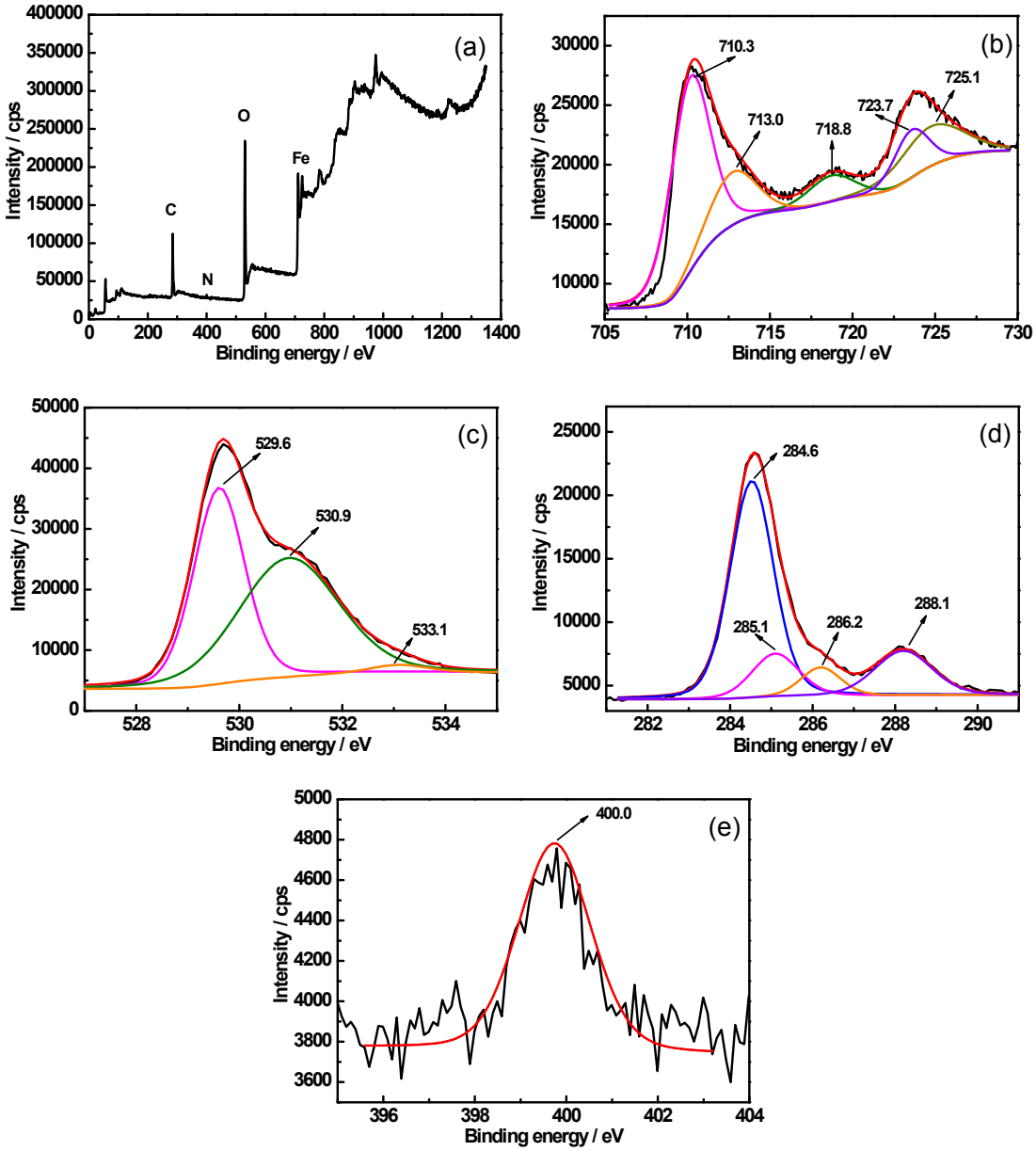

Fig. S11. XPS results of Fe_3O_4-PNIPAm nanoparticles. (a) Survey scan, (b) Fe 2p, (c) O 1s, (d) C 1s and (e) N 1s.

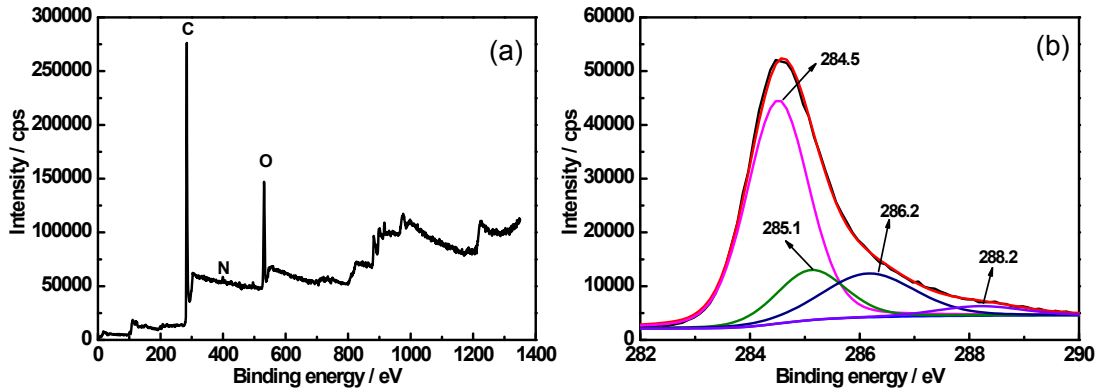

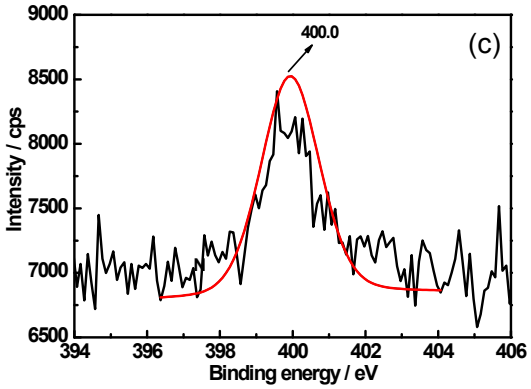

Fig. S12. XPS results of PS-PNIPAm nanoparticles. (a) Survey scan, (b) C 1s and (c) N 1s.

XPS analyses were used to investigate the composition of Fe_3O_4-PNIPAm and PS-PNIPAm nanoparticles (Fig. S11 and S12). For Fe_3O_4-PNIPAm nanoparticles, survey scan of Fig. S11a reveals the elements of Fe, C, N and O. In Fig. S11b, Fe $2p_{3/2}$, Fe $2p_{1/2}$ and satellite peaks of iron oxides locate at 710.3, 725, 718.8 eV.[26] A peak at 713.0 eV indicates the presence of FeOOH. O 1s spectrum (Fig. S11c) shows the oxygen atoms of iron oxide (529.6 eV), C=O (530.9 eV) and C–OH (533.1 eV).[26,27] Fig. S11d shows five components of $–CH_3$ (284.5 eV), –C–C=O (285.1 eV), C–N (286.2 eV), and HN–C=O (288.2 eV), indicating the presence of amide functionality.[10,11] The amide component is further confirmed by the N 1s peak located at 400.0 eV (Fig. S11e). For PS-PNIPAm nanoparticles, survey scan in Fig. S12a shows the elements of C, N and O. Five peaks ascribed to $–CH_3$ (284.5 eV), –C–C=O (285.1 eV), C–N (286.2 eV), and HN–C=O (288.2 eV) are observed in the C 1s spectrum of Fig. S12b. These peaks are assigned to poly(*N*-isopropylacrylamide). In addition, N 1s spectrum also shows the amide component (HN–C=O) at 400.0 eV (Fig. S12c). The above results suggest the presence of poly(*N*-isopropylacrylamide) on these nanoparticles.

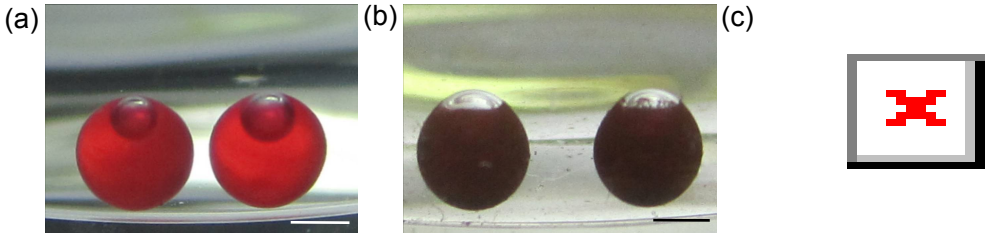

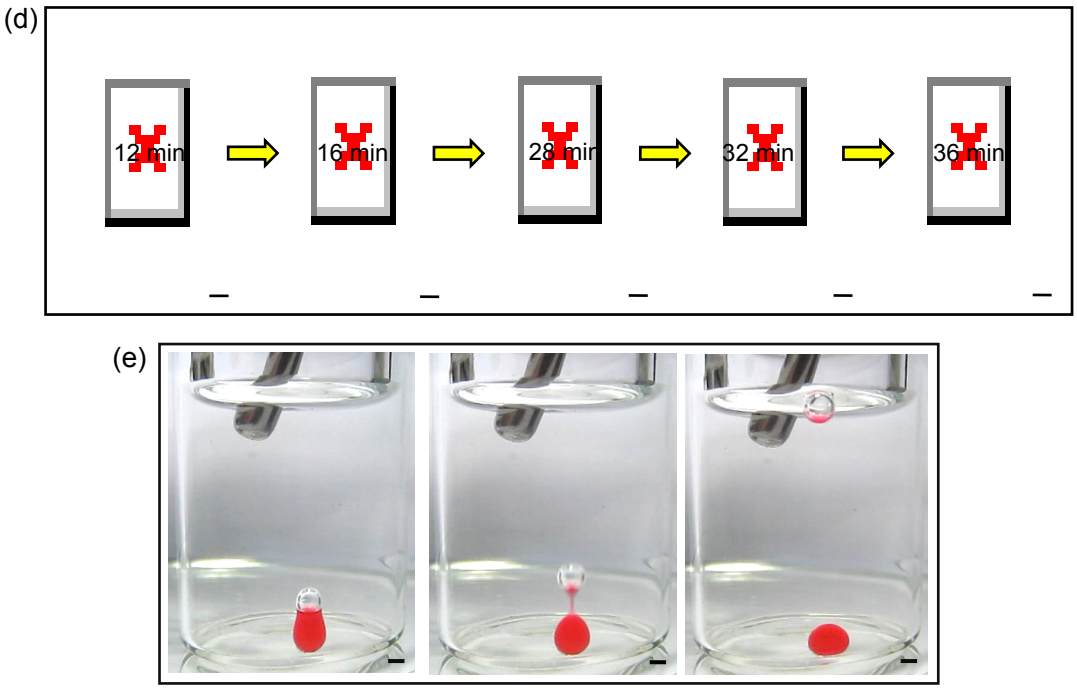

Fig. S13. Optical images for $CHCl_3$ droplets encapsulated with (a) PS-PNIPAm and (b) Fe_3O_4-PNIPAm nanoparticles; (c) CCl_4 droplets encapsulated with SiO_2-PNIPAm nanoparticles. These droplets were placed in water at 33.0 °C for 10 min. Scale bar: 1 mm. (d) Transportation of the encapsulated $CHCl_3$ droplets with different sizes in water at 33.0 °C. The volumes of $CHCl_3$ droplet from left to right were 6, 10, 20 and 35 μL, respectively. For clear observation, the droplets were removed once they reached the water surface. Scale bar: 2 mm. (e) Failure transportation of an encapsulated $CHCl_3$ droplet larger than 4.2 mm in diameter (40 μL). Scale bar: 2 mm.

Calculation of critical size of "airbag" for transporting a $CHCl_3$ droplet

It is accepted that an encapsulated $CHCl_3$ droplet will keep still in water until the buoyancy force is greater than its weight. Therefore, the critical size of bubble (or "airbag") for transporting a $CHCl_3$ droplet can be calculated through Eq. 1.

$$\rho_w(V_o + V_b)g \geq \rho_o V_o g \qquad (1)$$

Where ρ_w and ρ_o are the density of water and $CHCl_3$, respectively; V_o and V_b are the volume of the $CHCl_3$ droplet and bubble, respectively; g is the gravity constant. Here, we neglect the mass of the encapsulating nanoparticles and bubble. Then the critical volume of bubble is given by Eq. 2,

$$V_b \geq (\rho_o/\rho_w - 1)V_o \qquad (2)$$

Eq. 2 indicates that an "airbag" has ~1/2 volume of a $CHCl_3$ droplet can provide sufficient buoyancy force for the transportation. In this study, $CHCl_3$ droplets with volumes of 6, 10, 20 and 35 μL could transport in water at 33 ^oC (Fig. S13d). However, the effectiveness of this equation is strongly dependent on the mechanical durability (especially tensile strength) of the encapsulating layer. If the mass of a $CHCl_3$ droplet exceeds the tensile strength of its encapsulating layer, the resulting "airbag" cannot lift the droplet to the water surface. In fact, a $CHCl_3$ droplet larger than 4.2 mm (40 μL) failed to transport in water at 33 ^oC due to the isolation of its "airbag", as shown in Fig. S13e. Therefore, increasing the mechanical durability of an encapsulating layer will greatly improve the transportation capability of this bubble-induced strategy.

REFERENCES

1. S. L. Chen, P. Dong, G. H. Yang and J. J. Yang, *J. Colloid Interface Sci.*, 1996, **180**, 237−241.

2. N. Chen and Q. Pan, *ACS Nano*, 2013, **7**, 6875−6883.

3. S. Gu, T. Mogi and M. Konno, *J. Colloid Interface Sci*., 1998, **207**, 113−118.

4. H. Deng, X. L. Li, Q. Peng, X. Wang, J. P. Chen and Y. D. Li, *Angew. Chem., Int. Ed.*, 2005, **44**, 2782–2785.

5. C. Wang, N. T. Flynn and R. C. Langer, *Adv. Mater.*, 2004, **16**, 1074–1079.

6. P. Aussillous and D. Quéré, *Nature*, 2001, **411**, 924–927.

7. Y. Chu, Z. Wang and Q. Pan, *ACS Appl. Mater. Interfaces*, 2014, **6**, 8378−8386.

8. Q. Zhu and Q. Pan, *ACS Nano*, 2014, **8**, 1402–1409.

9. P. Calcagnile, D. Fragouli, I. S. Bayer, G. C. Anyfantis, L. Martiradonna, P. D. Cozzoli, R. Cingolani and A. Athanassiou, *ACS Nano*, 2012, **6**, 5413–5419.

10. H. Tu, C. E. Heitzman and P. V. Braun, *Langmuir*, 2004, **20**, 8313–8320.

11. X. Tai, J. H. Ma, Z. Du, W. Wang and J. Wu, *Powder Technol.*, 2013, **233**, 47–51.

12. G. Ju, M. Cheng, M. Xiao, J. Xu, K. Pan, X. Wang, Y. Zhang and F. Shi, *Adv. Mater.*, 2013, **25**, 2915–2919.

13. H. Yang, H. Zhu, M. M. R. M. Hendrix, N. J. H. G. M. Lousberg, G. D. With, A. C. C. Esteves and J. H. Xin, *Adv. Mater.*, 2013, **25**, 1150–1154.

14. H. G. Schild, *Prog. Polym. Sci.*, 1992, **17**, 163–249.

15. Z. M. O. Rzaev, S. Dincer and E. Piskin, *Prog. Polym. Sci.*, 2007, **32**, 534–595.

16. C. de las H. Alarcón, S. Pennadam and C. Alexander, *Chem. Soc. Rev.*, 2005, **34**, 276–285.

17. S. U. Pickering, *J. Chem. Soc. Trans.*, 1907, **91**, 2001–2021.

18. A. Böker, J. He, T. Emrick and T. P. Russell, *Soft Matter*, 2007, **3**, 1231–1248.

19. Y. Kaneko, K. Sakai, A. Kikuchi, R. Yoshida, Y. Sakurai and T. Okano, *Macromolecules*, 1995, **28**, 7717–

7723.

20. L. Liang, X. Feng, J. Liu and P. C. Rieke, *J. Appl. Polym. Sci*., 1999, **72**, 1–11.

21. E. S. Matsuoand and T. Tanaka, *J. Chem. Phys*., 1988, **89**, 1695–1703.

22. M. Shibayama and K. Nagai, *Macromolecules*, 1999, **32**, 7461–7468.

23. T. Okajima, I. Harada, K. Nishio and S. Hirotsu, *J. Chem. Phys*., 2002, **116**, 9068–9077.

24. H. Tokuyama and A. Kanehara, *Langmuir*, 2007, **23**, 11246–11251.

25. Y. Kaneko, R. Yoshida, K. Sakai, Y. Sakurai and T. Okano, *J. Membr. Sci*., 1995, **101**, 13–22.

26. D. Zhang, Z. Liu, S. Han, C. Li, B. Lei, M. P. Stewart, J. M. Tour and C. Zhou, *Nano Lett.*, 2004, **4**, 2151–2155.

27. C. Cheng, J. Lehmann, J. E. Thies, S. D. Burton and M. H. Engelhard, *Org. Geochem.* 2006, **37**, 1477–1488.